Journal of the Korean Nuclear Society
Volume 30, Number 6, pp.541~554, December 1998

COSMOS : A Computer Code for the Analysis of LWR UO_2 and MOX Fuel Rod

Yang-Hyun Koo, Byung-Ho Lee, and Dong-Seong Sohn
Korea Atomic Energy Research Institute
P.O.BOX 105 Yusong Taejon 305-600, Korea

(Received November 27, 1997)

Abstract

A computer code COSMOS has been developed based on the CARO-D5 for the thermal analysis of LWR UO_2 and MOX fuel rod under steady-state and transient operating conditions. The main purpose of the COSMOS, which considers high burnup characteristics such as thermal conductivity degradation with burnup and rim formation at the outer part of fuel pellet, is to calculate temperature profile across fuel pellet and fission gas release up to high burnup. A new mechanistic fission gas release model developed based on physical processes has been incorporated into the code. In addition, the features of MOX fuel such as change in themo-mechanical properties and the effect of microscopic heterogeneity on fission gas release have been also taken into account so that it can be applied to MOX fuel. Another important feature of the COSMOS is that it can analyze fuel segment refabricated from base irradiated fuel rods in commercial reactors. This feature makes it possible to analyze database obtained from international projects such as the HALDEN and RISO, many of which were collected from refabricated fuel segments. The capacity of the COSMOS has been tested with some number of experimental results obtained from the HALDEN, RISO and FIGARO programs. Comparison with the measured data indicates that, although the COSMOS gives reasonable agreement, the current models need to be improved. This work is being performed using database available from the OECD/NEA.

1. Introduction

Fuel rod performance codes are extensively used by fuel manufacturers, designers and licensing authorities for the analysis of in-reactor behavior of fuel rods. In recent years, some theoretical modeling has made a major contribution to the successful evolution of fuel analysis codes. However, there are increasing demands for a detailed understanding of the thermal, mechanical, physical and chemical processes governing the fuel rod behavior during normal reactor operation, for design basis accidents or severe accidents of extremely low probability. In addition, it is necessary to take into account the recent experimental findings such as rim effect and

thermal conductivity degradation with burnup. Moreover, modern fuel rod performance code needs to be flexible enough to allow for an easy modification of existing physical models or of material data as well as for the incorporation of new ones.

Up to now, KAERI has been using a computer code CARO-D5 developed by KWU for the analysis of UO_2 fuel [1]. The CARO-D5, whose models and characteristics are described in detail in Ref.2, has the following restrictions to be applied to high burnup UO_2 and MOX fuel. First, it does not consider high burnup phenomena such as degradation of thermal conductivity with burnup and the formation of rim structure at the outer part of fuel pellet. This feature, therefore, gives lower fuel temperature at high burnup leading to inaccurate thermal analysis. Second, an empirical fission gas release model is used in this code rather than mechanistic one, which makes it difficult to analyze the gas release and its effect on gap conductance mechanistically. These two features put restrictions on using this code for the analysis of high burnup UO_2 fuel because it does not provide adequate temperature profile across fuel pellet that is the starting point for the in-pile analysis of fuel. In addition, the code is used only for UO_2 fuel and not for MOX fuel. It is generally known that in-reactor behavior of LWR MOX fuel is similar to that of UO_2 fuel except that the addition of about less than 10 wt% of Pu to UO_2 matrix causes slight changes in the thermo-mechanical properties, radial power depression and fission gas release behavior of MOX fuel [3]. Therefore, many fuel vendors and utilities are using the same computer code to analyze both UO_2 and MOX fuel by considering these differences.

With these things in mind, a computer code COSMOS has been developed that can be utilized for the analysis of both UO_2 and MOX fuel up to high burnup. The COSMOS uses the same models as the CARO-D5 for heat transfer between pellet and cladding, pellet dimensional variation due to densification and swelling, change in gap size due to pellet fragments' relocation, and cladding growth and oxidation. However, the COSMOS contains new models to overcome the above-mentioned deficiencies of the CARO-D5. First, the COSMOS takes into account the high burnup phenomena such as rim effect and thermal conductivity degradation with burnup. Second, a mechanistic fission gas release model has been developed and incorporated into the code. Finally, MOX characteristics resulting from the addition of small amount of Pu has been considered so that the COSMOS can be also used for the MOX fuel.

Another important feature of the COSMOS, which can be used in PC, is that it can analyze the fuel segments refabricated from base irradiated fuel rods. This feature is established by storing all the relevant data of each axial segment and radial ring at the end of base irradiation and then using them as the initial conditions for refabricated fuel rods. They are usually tested in the experimental reactors that are equipped with measuring devices such as thermocouple and pressure gauge. The feature makes it possible to utilize the databases obtained from international projects such as HALDEN and RISO, many of which were collected from refabricated fuel segments.

2. Rim Effect and Thermal Conductivity Degradation

During about last ten years or so, there have been many experimental findings showing that thermal conductivity degrades with burnup and rim structures are formed at the outer part of fuel pellet at high burnup. These two phenomena are very important in terms of thermal analysis because they cause fuel

Table 1. Thermal Conductivity Correlation for MATPRO, SIMFUEL, and HALDEN [22]

MATPRO	$k = 1/(0.4378 + 2.294\times10^{-4}T) + 1.429 \times 10^{-2} \cdot e^{-1.876\times10^{-3}\cdot T}$
SIMFUEL	$k = 1/(0.432 + 0.0153 \cdot BU + (0.202 + 0.0025 \cdot BU)\times10^{-3}T)$
HALDEN	$k=1/(0.1148 + 0.0030 \cdot BU+2.475\times10^{-4} \cdot T)+0.0132 \cdot e^{-0.00188 \cdot T}$

temperature to increase significantly at high burnup fuel. Consequently, it would lead to enhanced fission gas release and then rod internal pressure yielding the possibility that fuel design criterion that fuel-to-clad gap should not be reopened could be violated.

The rim region, which acts as thermal barrier in the periphery of pellet, develops by Pu production and fissioning in low temperature. Using Lee et al.' s correlation for thermal conductivity, which is described in detail in Ref.4, temperature distribution in high burnup fuel is analyzed. This correlation has been developed using the following procedure. First, rim burnup is calculated based on rod average burnup using the formula $BU_{Rim}=1.43BU_{avg}$, where BU_{Rim} is the rim burnup and BU_{avg} is the pellet average burnup. A rim to average burnup ratio of 1.43 is derived from the measured data in RISO project [5]. Then rim width, which is another characteristic of rim region, is estimated from the measured data based on rim burnup. The least square method using linear relationship yields the following formula between rim width and rim burnup: $R_{Rim} = 5.24\ BU_{Rim} - 305.8$, where is the rim width in μm. Second, porosity in the rim region is calculated using the assumption that all the fission gases produced in the rim region exist as pores [6]. Finally, thermal conductivity in the rim region is obtained using the assumption that the rim region consists of pores and fully dense material of UO_2 fuel. The dependence of thermal conductivity on porosity is given as follows:

$$k_{Rim} = k_0 \cdot \left\{ \left[1 - a \cdot P_{Rim}^{\frac{2}{3}} \right] \cdot \left[1 - \frac{1}{1 + \frac{1}{a} \cdot P_{Rim}^{\frac{1}{3}} \cdot (k_o / k_p - 1)} \right] \right\} \quad (1)$$

where k_{Rim} = thermal conductivity of the porous rim (W/m • K),

k_0 = thermal conductivity of the fully dense material (W/ m • K),
$= k/[1-(2.58-0.58\times10^{-3}T)P]$,

k = thermal conductivity at 95% theoretical density,
$= 1/(A + B \cdot BU + C \cdot T)+f(T)$,

T = fuel temperature (℃),

P = porosity of fuel (volume fraction of the porous phase),

P_{Rim} = porosity of the rim region,

Bu = fuel burnup (MWd/kgU)

$f(T)$ = thermal conductivity due to electron excitation,

k_p = thermal conductivity of the pore (W/ m • K),
$= k_{Xe} = 0.72 \times10^{-4} \cdot (T+273)^{0.79}$ [7],

a = anisotropy factor (a=1 means isotropic pore distribution).

In the pellet interior region where rim characteristics does not exist, k is also calculated using the above formula with porosity corresponding to its region. In addition, thermal conductivity degradation with burnup is considered by adding the term $B \cdot BU$ in the denominator of k, which is the correlation for thermal conductivity at 95% theoretical density.

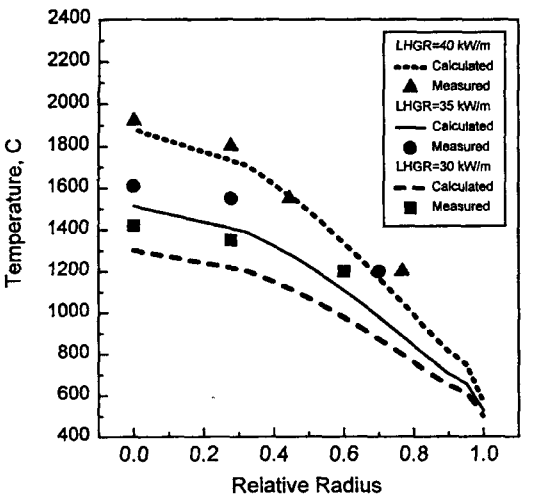

Fig. 1. Comparison of Measured and Calculated Temperature Profile for RISO-Ⅲ Experiment

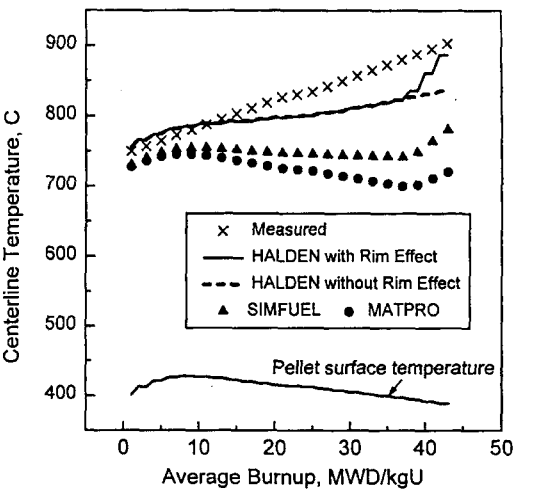

Fig. 2. Comparison of Measured and Calculated Centerline Temperature for UO_2 Fuel at the Linear Heat Rate of 25kW/m

MATPRO, SIMFUEL and HALDEN' s correlations for thermal conductivity at 95% theoretical density, which are given in Table 1, have been adopted and combined with the above formula. Then k_{Rim} has been incorporated into the COSMOS to compare the calculated and measured fuel centerline temperature.

Fig.1 shows the analysis results for the RISO data whose linear heat rate was 30, 35 and 40 kW/m, respectively, at the pellet average burnup of 43.5 MWd/kgU. Reasonable agreement is obtained for the linear heat generation rate of 40 kW/m with additional temperature jump being observed at the outer part of fuel. On the other hand, for 30 and 35 kW/m, the calculated temperatures are about 100℃ lower than the measured ones across fuel pellet. At present, it is considered that this discrepancy comes from the uncertainty in the gap conductance used in the present analysis. According to the recommendation of Bagger et al. [8], a value of 1.0 W/cm^2 • K, which is often considered appropriate for the situation when the gap is closed, was used as the gap conductance in the present calculation. Therefore, it is very likely that the gap conductance of 1.0 W/cm^2 • K used is higher than the real value leading to lower temperature in the fuel pellet. Another possible explanation for the discrepancy is that densification and swelling behavior of the tested fuel, which is very dependent upon manufacturing process and therefore microstructure of fuel pellet, was different from those assumed for the present analysis. Solid swelling (volume expansion of fuel due to solid fission products) rate of 0.40 % per 10^{20} fissions/cm^3 and maximum volume reduction of 3.44 % due to densification were used, respectively, for this analysis.

Fig.2 gives the measured centerline temperature in a HALDEN experiment at 25 kW/m as a function of fuel average burnup. It shows that centerline temperature increases linearly with burnup implying conductivity degradation, while the calculated result displays complicated trend since the gap conductance is affected by both gap size and fission gas release. However, substantial

increase in fuel temperature after 40 MWd/kgU indicates that rim region has been formed at pellet edge. In the early stage of irradiation, good agreement exists between the measurement and calculation when the HALDEN' s correlation, which considers the conductivity degradation, is used. Although the agreement is reasonable at the earlier and later stage of irradiation, a maximum deviation of about 50℃ exists at 40 MWd/kgU. As mentioned above, this difference is likely to result from the lack of accurate information on swelling and densification of the tested fuel rod. However, from this comparison, it can be concluded that the thermal conductivity developed in this paper could predict more reasonable fuel temperature for high burnup fuel when it is combined with the HALDEN' s correlation for a fuel of 95% theoretical density.

3. Fission Gas Release Model

3.1. Steady-State Model

Fission gas release model used in the COSMOS is a new mechanistic model developed Koo and Sohn [9]. The model was developed based on the assumption that a grain face is composed of 14 identical circular faces and a grain edge bubble can be represented by a triangulated tube around the circumference of three circular grain faces. The main features of the model are as follows:

- diffusion of gas atoms from grain interior to grain boundary
- precipitation of gas atoms into matrix and intergranular gas bubbles
- resolution of gas atoms from matrix and intergranular gas bubbles
- fission gas release due to bubble interconnection at grain boundary
- fission gas release due to recoil and knock-out and through open pore
- fission gas release at high burnup due to rim formation
- sweeping of gas atoms by grain growth

Both matrix and intergranular bubbles are assumed immobile in the model and their respective number densities are given as a function of fuel temperature. Extent of interlinkage of gas bubbles at grain boundary is assumed proportional to the swelling of gas bubbles at grain edge. An analytical solution gives the gas release rate from matrix to grain boundary, which considers the reinjection of fission gas atoms from grain face bubbles into matrix through the action of irradiation induced resolution.

3.2. Transient Model

3.2.1. Release due to Microcracking

According to many experiments performed during transient conditions, additional fission gas release during power change is observed. Analysis of the experimental results for transient fission gas release has shown that there exists a considerable fission gas burst in case of both power increases [10] and power reductions [11,12]. These two effects can be explained in terms of the microcracking where changes in the stresses within the fuel cause grain boundaries to tear apart where fission gases are stored. Since this mechanism is not a thermally activated process, it simply requires a specific temperature level beyond which the stresses only change appreciably. Based on Hering' s work [13], it is assumed in the present model that all the fission gases retained in the grain boundaries are released instantaneously to free space due to microcracking if the following conditions are satisfied, where q' is the linear power for the axial node and T is the ring

temperature:

Case 1 : When the linear power increases from q'_1 to q'_2 leading to temperature increase from T_1 to T_2, microcracking takes place if $q'_2 - q'_1 > 35$ W/cm, $q'_2 > 300$ W/cm and $T_2 > T_g$,. Here the burnup dependent threshold temperature T_g is defined by $T_g = 1500\ (1-Bu/80)$, where T_g is in ℃ and Bu is in MWd/kgU.

Case 2 : When the linear power decreases from q'_1 to q'_2 leading to temperature reduction from T_1 to T_2, microcracking takes place if $q'_1 - q'_2 > 35$ W/cm, $q'_1 > 300$ W/cm and $T_1 > T_g$, The burnup dependent threshold temperature T_g is the same as in the Case 1.

Case 3 : Microcracking takes place if $q' > 300$ W/cm and $T > T_g$ in the last time interval of power history.

3.2.2. Additional Release During Power Transient

The fission gas release rate from the matrix to the grain boundary derived by Koo and Sohn [9] is only valid under steady-state operating conditions. This means that the differential equation for gas release rate from grain interior to grain boundary was solved under the assumption that power (temperature) does not change or change slightly over time. This assumption is no longer valid for power transients where power changes rapidly over a short time interval. An exact mathematical analysis implies that in the case of relatively rapid transient an additional term has to be included for the solution for gas release rate from grain interior to grain boundary. However, this would involve very complex and considerable effort. For this reason, an empirical equation describing the additional contribution to gas transport from the grain to grain boundary is selected for use in the model. In contrast with gas release due to microcracking, this mechanism is activated only when power increases. This is obvious because gas diffusion coefficient increases only when power increases leading to additional gas release compared with steady-state conditions. In the model, it is assumed that additional gas release under transient conditions takes place if the first condition (Case 1) in Sec.3.2.1 is satisfied. The additional released amount ΔG_T is given by $F_T G_M$, where $F_T=(T-T_g)/1000 \leq 0.3$ and G_M is the momentary gas inventory in the grain interior when the power increase occurs.

Calculations were carried out for the AN3 and AN4 fuel segments refabricated from ANF fuel with pressure transducers and fuel centerline thermocouples installed [8]. The ANF fuel was of PWR design and had been irradiated in the Biblis-A reactor (Germany) to a rod average burnup of about 40 MWd/kgU. The highest linear heat rating seen by this fuel was 26.7 kW/m. The fuel did not release more than 0.3 % of their fission gas inventory during its base irradiation. The restructuring was found negligible too.

Fuel centerline temperature and relative fission gas release observed for the AN3 and AN4 fuel segments during transient test in the DR3 reactor at RISO are compared with calculation results in Figs.4 and 5, respectively. The main difference between these two fuel segments was the initial gas filling. The AN3 fuel segment was filled with 15 bar helium and AN4 fuel segment was filled with one bar xenon.

3.2.3. Comparison and Discussion

The model' s capacity for commercially irradiated fuel rods has been tested with the KWU' s database, which covers very wide range of steady-state and transient operating conditions. Rod average burnup reaches up to 51 MWd/kgU

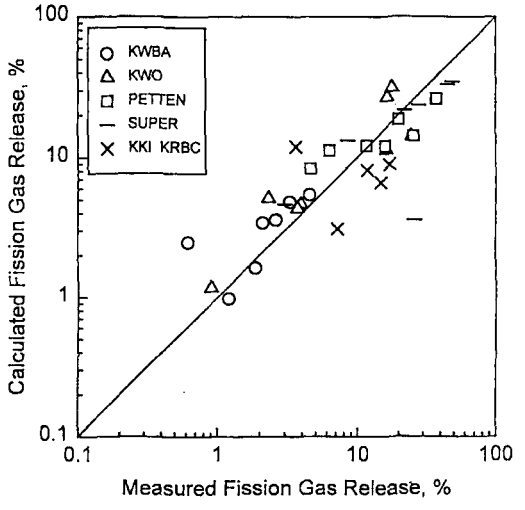

Fig. 3. Comparison of Measured and Calculated Fission Gas Release

and linear heat rate up to 490 W/cm. Fig.3 shows the comparison between the calculated and measured fission gas release. The improvement of the model will be done continuously with the HLADEN, HBEP and RISO database.

The COSMOS' s another feature, which is its capacity of analyzing fuel segments refabricated from base irradiated fuel rods, has been also tested with the RISO' s data obtained from AN3 and AN4 fuel segments [8]. The centerline temperatures of these segments were measured with a thermocouple inserted at the top of the fuel stack in a 2.5 mm diameter. Since the temperature measurement was made for an annular fuel pellet having an inner diameter of 2.5 mm, correction has been made to convert this value to the corresponding one in a solid fuel pellet using the method given in Ref.8. The assumption that fuel thermal conductivity and volumetric heat generation rate are unchanged across pellet radial direction was used in the correction. It was found that the corrected temperatures for solid pellet were 275~280° C higher than the measured ones. The dotted lines in Figs.4(a) and 5(a) represent the corrected centerline temperatures. As in Sec.2, in the present analysis gap conductance was assumed to be 1 $W/cm^2 \cdot K$ for the situations when the gap is closed.

In addition, it should be noted that in calculating the fuel temperature, thermal conductivity degradation with burnup was considered with using the Lee et al.' s correlation [4]. In case of the AN3 fuel segment the difference between the calculated and measured fuel centerline temperature are about 0~100° C. The same argument can be applied for explaining this discrepancy as used for Fig.1; that is, it is implied that the assumed gap conductance of 1 $W/cm^2 \cdot K$ is higher than the real gap conductance. In the same way, the calculated centerline temperature is shown to be lower than the measured one for the AN4 fuel segment.

Fission gas release during power change depends on temperature, power conditions and fuel burnup when power change occurs. In addition, it depends on the amount of fission gas stored in the grain interior and grain boundary during steady-state operation. Therefore, the prerequisite for the accurate prediction of fission gas release during power change is to predict the amount of fission gas stored in the grain interior and grain boundary accurately. In this paper, Koo and Sohn' s steady-state fission gas release model [6] was used to calculate the amount of fission gas deposited in the grain interior and grain boundary. Figs.4(b) and 5(b) show that the calculated release kinetics yields reasonable agreement with the measured one. However, in both cases there is about 10% difference at maximum during both the stages of power increase and hold at high power. According to Morgan et al. [14], there existed athermal gas release of 6~7% at a low power of 11 kW/m due to fabrication characteristics specific to the AN3 and AN4 fuel segments, which

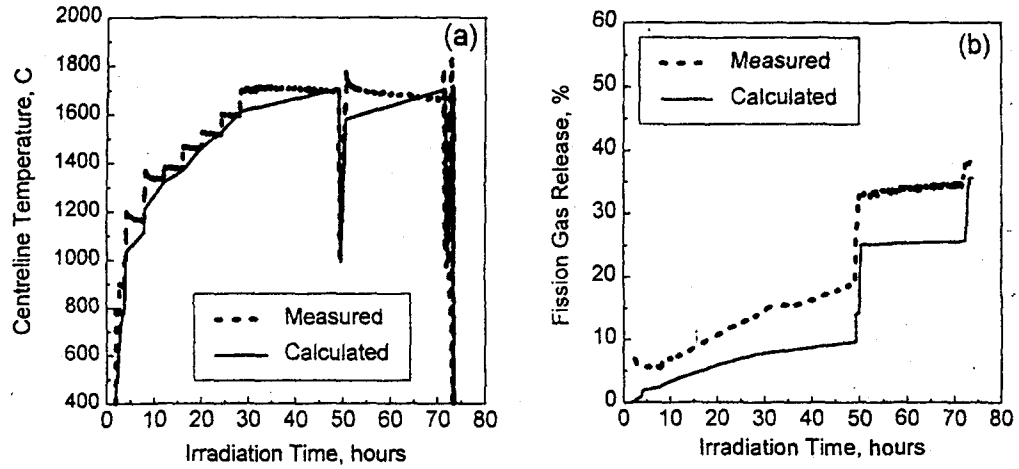

Fig. 4. Comparison of Measured and Calculated (a) Centerline Temperature and (b) Fission Gas Release for AN3 Case Performed in RISO-Ⅲ Experiment

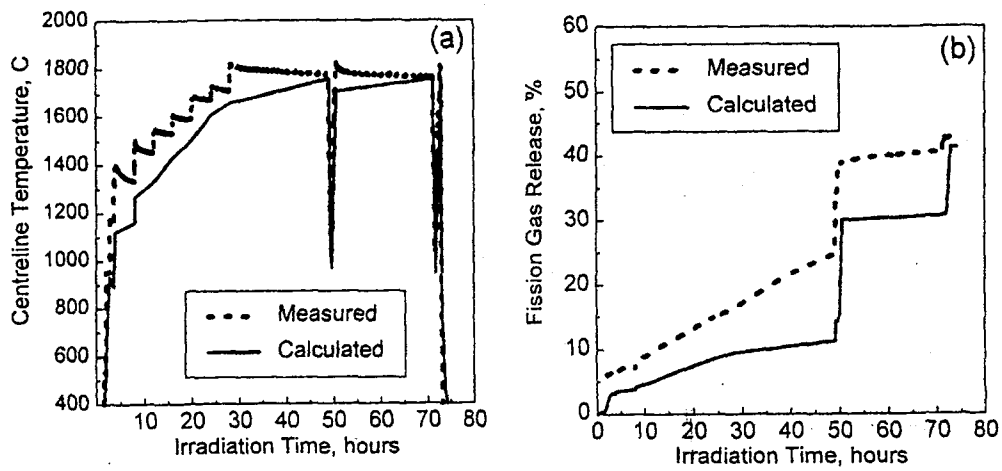

Fig. 5. Comparison of Measured and Calculated (a) Centerline Temperature and (b) Fission Gas Release for AN4 Case Performed in RISO-Ⅲ Experiment

is an unusual phenomenon that is difficult to model. This rather high athermal gas release was found in low density fuels where fission gas may have been collected in the fabrication pores during steady-state irradiation and have been released to free spaces during power ramps through cracks.

4. MOX Feature

MOX fuel for LWR, which is being used extensively in the West Europe as a means of

disposing of stocked Pu and reducing spent LWR UO_2 fuel, is different from typical UO_2 fuel in that it contains a small amount of Pu from the beginning of irradiation. Due to the difference in pellet microstructure arising from the addition of Pu, the following features should be taken into account when a computer code for the analysis of MOX fuel is developed based on a computer code for UO_2 fuel. First, changes in the thermo-mechanical properties of MOX fuel compared with UO_2 fuel such as thermal conductivity and thermal expansion coefficient, specific heat capacity, and melting temperature should be considered. Second, change in radial power depression across fuel pellet should be taken into account because it determines the radial temperature profile that governs all the physical and chemical processes in the fuel. Third, effect of different microstructure on fission gas release, which is one of the main concerns for MOX fuel resulting from its higher power than UO_2 fuel at EOL because the reactivity of MOX fuel decreases more slowly with burnup.

4.1. Thermo-mechanical Properties

The following themo-mechanical properties of MOX fuel are different from those of UO_2 fuel depending on the amount of Pu added to the UO_2 matrix:

- thermal conductivity
- thermal expansion coefficient
- specific heat capacity
- melting temperature

In-reactor behavior of MOX fuel resulting from the differences in the above-mentioned properties was described in Ref.15. The most significant difference is found in the thermal conductivity. Out-of-file measurements have shown that thermal conductivity for MOX fuel are slightly lower than that for UO_2 fuel by about 10%. This gives rise to different radial temperature profile in fuel pellet in combination with different radial power depression.

4.2. Radial Power Depression

Radial power depression is very important because it determines the radial temperature profile that governs almost all the physical and chemical processes taking place in fuel rod. The computer program FACTOR [16] that has originally been developed for calculating the normalized power density and burnup factors for UO_2 fuel has been extended to MOX fuel and incorporated into the COSMOS. This program calculates the radial power depression in MOX fuel as a function of Pu fissile content from a detailed nuclear calculation [17]. As shown in Fig.6(a), MOX fuel has a higher radial power depression early in life due to the higher absorption cross section of Pu isotopes. This implies that, if operated at the same power, centerline temperature in MOX fuel would be lower than in UO_2 fuel. However, as burnup increases Pu isotopes build up higher in the periphery of UO_2 fuel because of the capture of epithermal neutrons in the resonances of ^{238}U, whereas the amount of Pu in the outer part of MOX fuel decreases by consumption. This makes the radial power distribution for the two types of fuel almost the same as shown in Fig.6(b). Therefore, only the difference in thermal conductivity produces the different radial temperature profile for the same power.

Using the FACTOR, the radial distribution of burnup has been calculated and compared for the fuels tested in RISO [18]. As seen from Fig.7, there is close agreement between the measurement and prediction. This implies that the radial power distribution in LWR fuel is well predicted by the FACTOR.

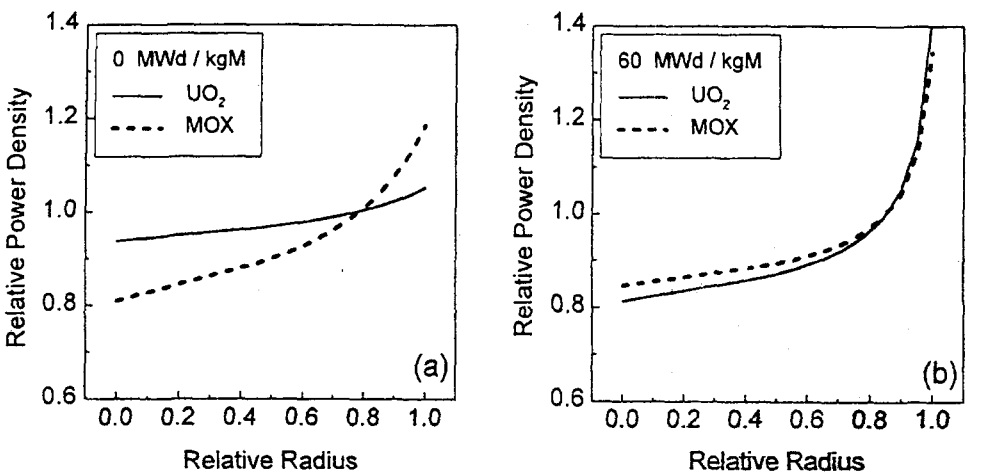

Fig. 6. Comparison of Relative Power Density at 0 and 60 MWd/kgM Between UO_2 Fuel(Enrichment : 3.5%) and MOX Fuel(Pu-Fissile : 3.5%)

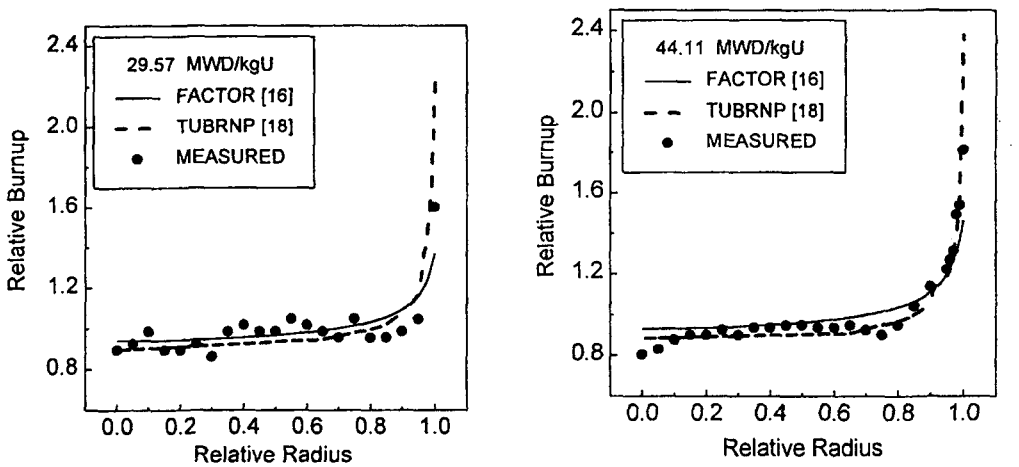

Fig. 7. Comparison of Measured Burnup Profile with that Calculated by FACTOR for UO_2 Fuel Rods Used in the RISO-Ⅲ Experiment

4.3. Fission Gas Release in MOX Fuel

Depending on the manufacturing method of MOX fuel, heterogeneity can exist in the microstructure of MOX fuel pellet due to the incomplete mixing of PuO_2 powder with UO_2 powder.

There are some controversies over whether fission gas release is enhanced in MOX fuel compared with UO_2 fuel under similar operating conditions. According to several experiments, there appears to be a little effect of microstructure on fission gas release in currently produced fuel. In addition, high gas release in MOX fuel results from

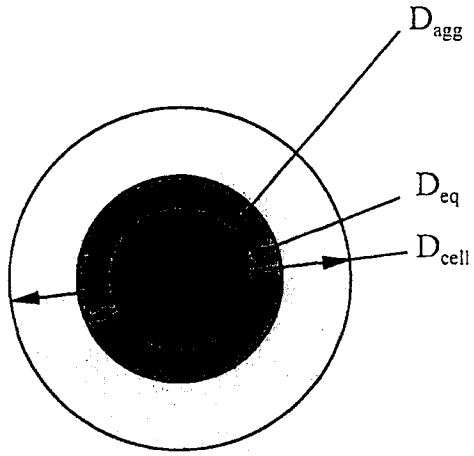

Fig. 8. The Equivalent Spherical Cell Model for Heterogeneous MOX Fuel

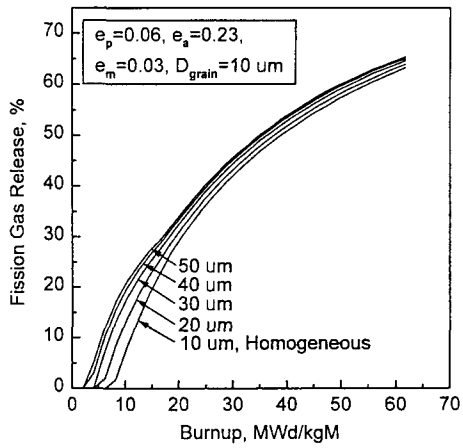

Fig. 9. Effect of Pu-rich Particle Size(D_{agg}) on Fission Gas Release in MOX Fuel at 1000℃

higher operating powers in MOX fuel later in life because reactivity falls more slowly with burnup. Therefore, it is necessary to take into account this effect in analyzing MOX fuel.

To analyze the effect of microscopic heterogeneity on fission gas release, an equivalent spherical cell model has been developed using the assumption that Pu-rich particles are distributed uniformly in UO_2 matrix [19]. An equivalent spherical cell is assumed to consist of an equivalent spherical particle with the diameter of $D_{eq} = D_{agg} + 2\ L_{rec}$ surrounded by the UO_2 matrix containing a Pu-rich particle, where D_{agg} is the average size of the Pu-rich particle and L_{rec} is the recoil length of fission products (see Fig.8). The recoil length is assumed to be 6 μm. In Fig.9, e_p is the average Pu content of the pellet, e_a is the Pu content of the Pu-rich particle, e_m is the Pu-content in the UO_2 matrix, and D_{grain} is the grain size of the UO_2 matrix. The diameter of an equivalent spherical particle is then defined as follows:

$$D_{cell} = D_{agg} \Big/ \sqrt[3]{\frac{e_p - e_m}{e_a - e_m}} \ . \qquad (2)$$

The fission rates in the equivalent spherical particle and matrix are calculated considering the effective Pu contents in each zone. When e_p, e_a, e_m, and D_{agg} are 0.06, 0.23, 0.038, and 13 μm, respecti-vely, the fission rate in the Pu-rich particle is seven times greater than that in the UO_2 matrix. The parameter e_m is calculated based on the assumption that the concentration of Pu-rich particles is $2\times10^{13}/m^3$. If the fuel parameters are such that D_{eq} is larger than D_{cell}, the fuel can be considered to be a homogeneous one.

The Pu content of the equivalent spherical particle is calculated as follows:

$$e_{eq} = e_m + \left(\frac{D_{agg}}{D_{eq}}\right)^3 \cdot (e_a - e_m) . \qquad (3)$$

Fission rates in the equivalent spherical particle and UO_2 matrix are given below, where the average fission rate F_{av} can be obtained from the average power density:

$$F_{eq} = \left(\frac{e_{eq}}{e_p}\right) \cdot F_{av} , \qquad (4)$$

$$F_m = \left(\frac{e_m}{e_p}\right) \cdot F_{av} . \qquad (5)$$

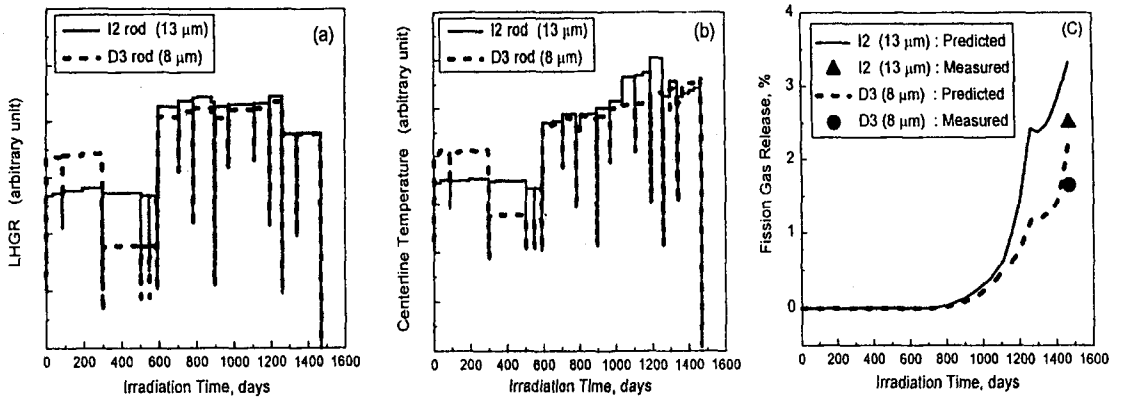

Fig. 10. (a) Irradiation Power Histories, (b) Fuel Centerline Temperatures, and (c) Fission Gas Releases for Two MOX Fuel Rods 12 and D3, Respectively

The average fission rates in each region are incorporated into the fission gas release model for UO_2 fuel described in Sec.3.1, and are used to calculate gas release in their respective region.

Fig.9 shows how the size of Pu-rich particle affects fission gas release in MOX fuel at 1000℃.

This model has been tested with use of the data obtained from the an international program [19]. Since these are proprietary information, only the arbitrary power histories and centerline temperatures for two MOX fuel rods I2 and D3 are shown in Fig.10(a) and (b), respectively. The two MOX rods manufactured by MIMAS process were irradiated in one Swiss reactor for five cycles. These fuel rods contained fuel pellets of different grain sizes of 15 and 8μm, respectively. Fig.10(c) displays the kinetics of fission gas release and compares the measured and calculated fission gas release for I2 and D3. The measured releases for I2 and D3 are 2.5 and 1.65%, respectively, whereas the calculated ones are 3.3 and 2.1%.

At the moment, only a small number of data points are available for irradiated MOX fuel to draw any definite conclusion about the validity of the present model. However, according to our another recent analysis, whose aim was to investigate the MOX fuel behavior during transient operating conditions in the HALDEN reactor, shows that the COSMOS yields reasonable agreement with the measured centerline temperatures and fission gas release converted from the measured rod internal pressure [20].

5. Conclusions

(1) A computer code COSMOS has been developed based on the CARO-D5 for the thermal analysis of UO_2 and MOX fuel rod under steady-state and transient operating conditions. The main purpose of the COSMOS is to calculate the temperature profile across fuel pellet and fission gas release up to high burnup considering high burnup characteristics such as thermal conductivity degradation with burnup and rim formation. A new mechanistic fission gas release model developed based on physical processes has been incorporated into the code.

(2) Features of LWR MOX fuel such as change in themo-mechanical properties, radial power depression and the effect of microscopic heterogeneity on fission gas release have been

also taken into account so that it can be applied to the analysis of MOX fuel.

(3) The capacity of the COSMOS for UO_2 fuel has been tested up to the rod average burnup of 51 MWd/kgU with some number of results obtained from the HALDEN and RISO experiments. Comparison with the measured data indicates that, although the COSMOS gives reasonable agreement, the current models need to be improved. This work is being performed using the database available from OECD/NEA [21], which includes many high burnup fuel rods.

(4) Concerning the analysis of MOX fuel, the COSMOS has been tested only with the data obtained from an international project. Comparison with the measured data indicates that the calculated centerline fuel temperature and fission gas release fraction show reasonable agreement with the measured ones. The COSMOS will be tested again in the future when more MOX data are accumulated in the HALDEN project.

(5) Another important feature of the COSMOS is that it can analyze fuel segments refabricated from base irradiated commercial fuel rods. This feature makes it possible to analyze database obtained from some international projects such as the HALDEN and RISO, many of which were collected from refabricated fuel segments.

6. References

1. R.Eberle, F.Wunderlich, and I.Distler, "CARO-D5: A Computer Code for LWR Fuel Rod and Its Application," KWU Technical Report B111/83/76, March 83.
2. R.Eberle, "Fuel Rod Modelling and Fuel Rod Code CARO-D5," March, (1986).
3. J.A.Turnbull, "A Review of MOX Fuel and Its Use in LWRs," HWR-435, Nov., (1995).
4. Byung-Ho Lee, Yang-Hyun Koo and Dong-Seong Sohn, "Development of a Thermal Conductivity Correlation for Pellet Rim Region and Its Application to the Analyses of Behavior of High Burnup Fuel," Technical Committee Meeting on advances in pellet technology for improved performance at high burnup, Tokyo, Japan, Oct.28 - Nov.1, (1996).
5. N. Kjaer-Pederson, "Rim Effect Observations from the Third RISO Fission Gas Report," Proceedings of a Technical Committee Meeting, Ontario, Canada, April 28, (1992).
6. Byung-Ho Lee, Yang-Hyun Koo, and Dong-Seong Sohn, "Dependence of Rim Porosity and Temperature Behavior in the High Burnup UO2 Fuel," Proceeding of the Korean Nuclear Society Autumn Meeting, Taegu, Korea, October (1997).
7. H. Kampf and G. Karsten, "Effect of Different Types of Void Volumes on the Radial Temperature Distribution of Fuel Pins," *Nuclear Application and Technology*, **9**, 288 (1970).
8. C.Bagger, M.Mogensen, and C.T.Walker, "Temperature Measurements in High Burnup UO2 Nuclear Fuel: Implications for Thermal Conductivity, Grain Growth and Gas Release," *J. Nucl. Mater.*, **63**, 11 (1994).
9. Yang-Hyun Koo and Dong-Seong Sohn, "Development of a Mechanistic Fission Gas Release Model for LWR UO_2 Fuel under Steady-State Conditions," *J. Kor. Nucl. Soc.*, **28**, 229 (1996).
10. R. Manzel, "The Fission Gas Release from High Burnup UO_2 Fuel Segment during Short Time Transients," KWU Technical Report B21/84/060a, June (1984).
11. P. Knudsen et al., "Final Report on the RISO Transient Fission Gas Release Project," RISO-TFGP-R29, May (1986).
12. F. Sontheimer, "First Results of RISO-III

Project," U641/88/066, April (1988).
13. W. Hering, "Description of the New Mechanistic Fission Gas Release Model," KWU work report, January (1989).
14. M. Morgan, C. Bagger, H. Toftegaard, P. Knudsen and C.T. Walker, "Observations of Athermal Gas Release from Water Reactor Fuel at Extended Burnup," J. Nucl. Mater., **202**, 199 (1993).
15. Yang-Hyun Koo, Byung-Ho Lee, and Dong-Seong Sohn, "Comparison of In-reactor Behavior of UO_2 and MOX Fuel," Proceeding of the Korean Nuclear Society Autumn Meeting, Seoul, Korea, October (1995).
16. Yang-Hyun Koo, Byung-Ho Lee, and Dong-Seong Sohn "FACTOR: A Program for Calculating the Radial Power Density and Burnup Factors in MOX and UO_2 Fuel," KAERI Internal Report, July (1996).
17. Hyung-Kook Joo, Department of Future Fuel Development, KAERI, private communication, Aug., (1996).
18. K. Lassmann, C. O' Carroll, J. van de Laar and C.T. Walker, "The Radial Distribution of Plutonium in High Burnup UO_2 Fuel," J. Nucl. Mater., **208**, 223 (1994).
19. An International Programme:Minutes of the Second Programme Committee Meeting," May, (1997).
20. Yang-Hyun Koo, Dong Seong Sohn, and P. Strijov, "A Fission Gas Release Model for UO_2 and MOX fuel," Unpublished work, June, (1998).
21. P.M.Chantoin, E.Sartori and J.A.Turnbull, "The Compilation of a Public Domain Database of Nuclear Fuel Performance for the Purpose of Code Development and Validation," OECD/NEA, IFPE Data Base, Version June, (1997).
22. KAERI/RR-1697/96, "Development of Design Technology for Future Fuel," KAERI, July, (1997).